Inorganic Chemistry

Article

pubs.acs.org/IC

Lanthanide(III) Di- and Tetra-Nuclear Complexes Supported by a Chelating Tripodal Tris(Amidate) Ligand

Jessie L. Brown,[†] Matthew B. Jones,[†] Andrew J. Gaunt,*[,†] Brian L. Scott,[‡] Cora E. MacBeth,*[,§] and John C. Gordon[†]

[†]Chemistry Division and [‡]Materials Physics and Applications Division, Los Alamos National Laboratory, Los Alamos, New Mexico 87545, United States

[§]Department of Chemistry, Emory University, Atlanta, Georgia 30322, United States

Supporting Information

ABSTRACT: Syntheses, structural, and spectroscopic characterization of multinuclear tris(amidate) lanthanide complexes is described. Addition of $K_3[N(o\text{-PhNC(O)}^t\text{Bu})_3]$ to LnX_3 (LnX_3 = $LaBr_3$, CeI_3, and $NdCl_3$) in *N*,*N*-dimethylformamide (DMF) results in the generation of dinuclear complexes, $[Ln(N(o\text{-PhNC(O)}^t\text{Bu})_3)(DMF)]_2(\mu\text{-DMF})$ (Ln = La (**1**), Ce (**2**), Nd(**3**)), in good yields. Syntheses of tetranuclear complexes, $[Ln(N(o\text{-PhNC(O)}^t\text{Bu})_3)]_4$ (Ln = Ce (**4**), Nd-(**5**)), resulted from protonolysis of $Ln[N(SiMe_3)_2]_3$ (Ln = Ce, Nd) with $N(o\text{-PhNCH(O)}^t\text{Bu})_3$. In the solid-state, complexes **1**−**5** exhibit coordination modes of the tripodal tris(amidate) ligand that are unique to the 4f elements and have not been previously observed in transition metal systems.

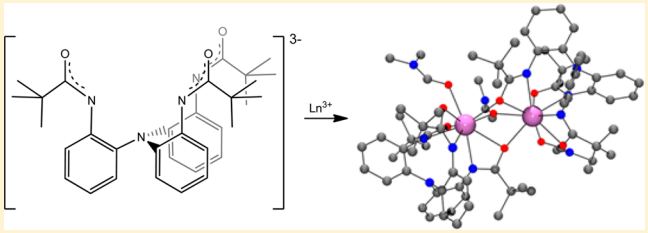

INTRODUCTION

There is a research need to elucidate the coordination chemistry of the f-elements with a wide range of ligand architectures and donors types. One aspect is to understand trends and changes in speciation and bonding due to the relevance that such knowledge can play in controlling and manipulating f-element behavior in various separation processes.[1−6] Rather than designing separation relevant ligands directly, one approach is to define the baseline chemical reactivity, complex structures, and bonding properties of the f-elements with different functional groups or donor types, such that should those chemical functionalities be incorporated into a separation agent or any process in the future then an understanding of the chemical interactions between metal and ligand will already exist.[7−13] Mixed N,O donor ligands have attracted recent attention due to their interesting bonding properties with the f-elements.[14−18] In this contribution, we focus on exploring the chemistry of several early lanthanide ions in the trivalent oxidation state with mixed N,O donor ligands. Surprisingly, although there are several examples of lanthanide complexes with simple amidate ligands,[19−30] the chemistry of the 4f ions with more complex amidate scaffolds has not been explored. We chose to study the tripodal ligand, $[N(o\text{-PhNC(O)R})_3]^{3-}$ (R = alky, aryl), which features an acyl substituted amidate moiety capable of wide synthetic modification and varied coordination chemistry (Chart 1).

MacBeth and co-workers have previously demonstrated diverse chemistry with a variety of tripodal tris(amidate) scaffolds with both the transition metals and main-block elements.[31−34] For example, addition of $N(o\text{-PhNHC(O)}^t\text{Bu})_3$ to $AlMe_3$ afforded $[Al(N(o\text{-PhNC(O)}^t\text{Bu})_3]$ which exhibited a chelating tris(κ^2-amidate) coordination mode for the tripodal ligand.[31] Similarly, *in situ* deprotonation of $N(o\text{-PhNHC(O)}^t\text{Bu})_3$ with potassium hydride (KH) in DMF, followed by transmetalation with $NiBr_2$ resulted in formation of $[Ni(N(o\text{-PhNC(O)}^t\text{Bu})_3]^-$. Interestingly, in the solid-state, the Ni(II) complex exhibits both *N*-amidate and *O*-amidate coordination modes, likely adopted to reduce steric strain afforded by the bulky *tert*(butyl) substituents.[32] Lastly, the diiron(II) complex, $[Ph_4P][KFe_2(N(o\text{-PhNC(O)}^i\text{Pr})_2]$, derived from the isopropyl substituted ligand, $N(o\text{-PhNHC(O)}^i\text{Pr})_3$, is supported via two μ-1,3-(κN:κO)-amidato ligands, where one pendant arm within each amidate ligand adopts a bridging coordination mode.[33] The versatile ligation modes and reactivity observed with the tripodal tris(amidate) ligand with the main group elements and the transition metals lent credence to the expectation that the 4f series of trivalent cations would be capable of supporting unique coordination modes and molecular assemblies.

Herein we report the syntheses, isolation, and characterization of a series of multinuclear Ln(III) (Ln = La, Ce, Nd) complexes with the multichelating tripodal ligand, $[N(o\text{-PhNC(O)R})_3]^{3-}$ (R = ^{t}Bu). These complexes can be obtained by either halide-salt metathesis or protonolysis, the latter utilizing $Ln[N(SiMe_3)_2]_3$ (Ln = Ce, Nd) as the precursor material. All reported complexes were structurally characterized by X-ray crystallography, as well as by ^{1}H NMR and IR spectroscopies. Preliminary reactivity studies of the Ln(III) complexes are also discussed.

Received: February 6, 2015
Published: April 6, 2015

DOI: 10.1021/acs.inorgchem.5b00299
Inorg. Chem. 2015, 54, 4064−4075

Chart 1. Possible Coordination Modes of Tripodal Amidate Ligands[a]

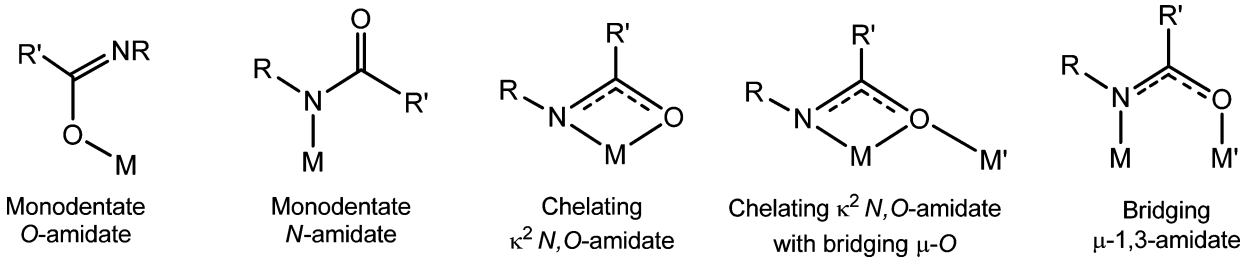

[a]Chart modified from ref 32.

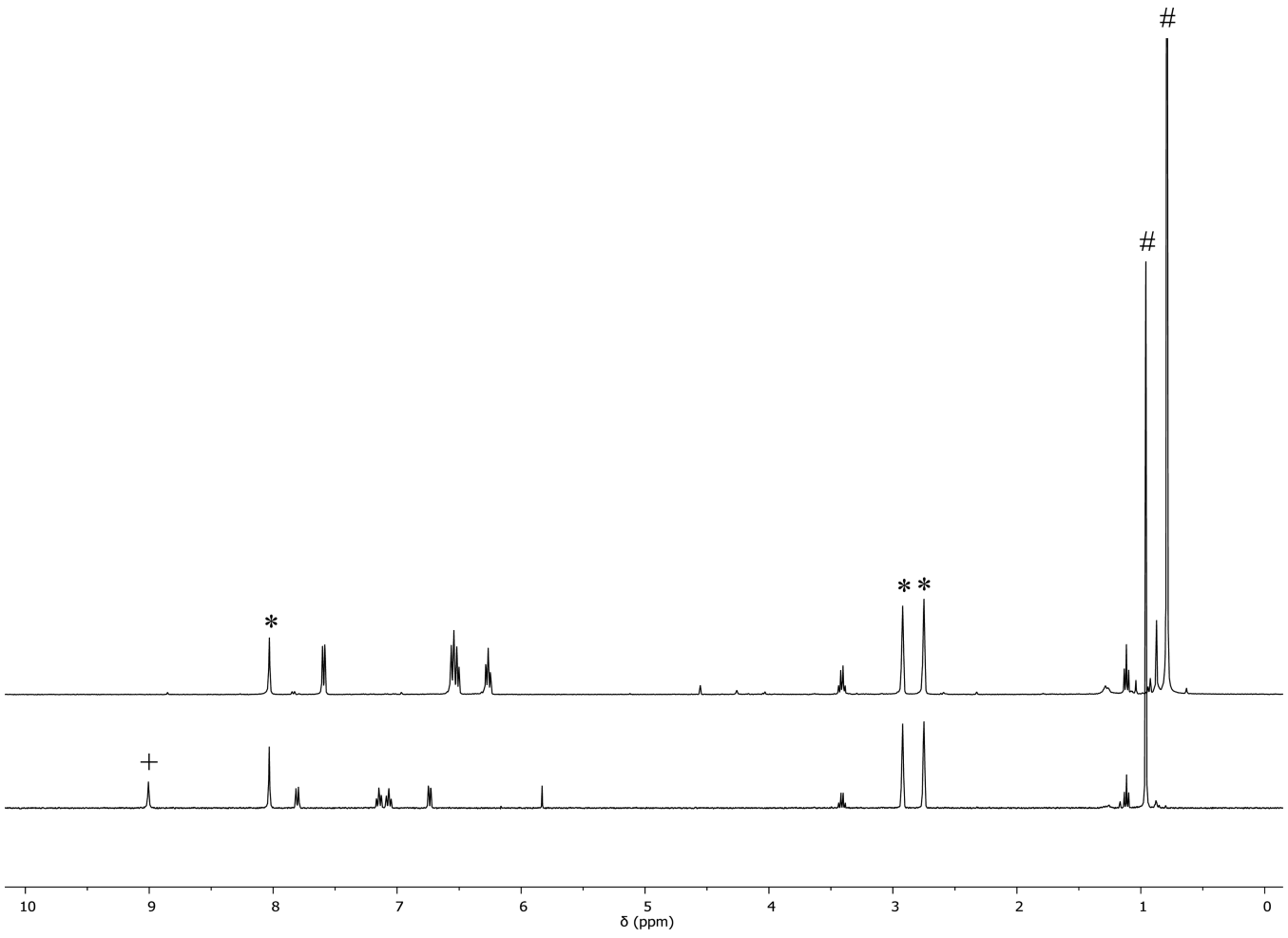

Figure 1. Overlay of the ^{1}H NMR spectra of H_3L^{tBu} in DMF-d_7 (bottom) and of the reaction between H_3L^{tBu} and KH after 5 h (top). The amide protons of H_3L^{tBu} are denoted by (+), while the ^{t}Bu protons are denoted by (#). Residual solvent signals of DMF are denoted by (*).

RESULTS AND DISCUSSION

Initial attempts to isolate the target complexes involved *in situ* deprotonation of the ligand, N(*o*-PhNHC(O)^{t}Bu)$_3$ (H_3L^{tBu}), with a slight excess of KH in DMF, followed by addition of 1 equiv of LnX_3 (LnX_3 = $LaBr_3$, $CeBr_3$, $NdCl_3$). Unfortunately, this synthetic strategy consistently results in complicated reaction mixtures. Specifically, H_3L^{tBu} persists as a major impurity as observed by ^{1}H NMR spectroscopy even upon multiple recrystallizations of the isolated materials. Changing the solvent medium to tetrahydrofuran (THF) or 1,2-dimethoxyethane (DME) was also not successful, due in large part to the poor solubility of the ligand and the lanthanide trihalide starting materials. To attempt to understand the deprotonation of H_3L^{tBu} and develop a cleaner synthetic method, the reaction between H_3L^{tBu} and excess KH in DMF-d_7 was monitored by ^{1}H NMR spectroscopy. A dominant product was observed after several hours, tentatively assignable to the potassium salt, K_3[N(*o*-PhNC(O)^{t}Bu)$_3$] (K_3L^{tBu}). Notably, the amide NH protons of H_3L^{tBu}, observed at 8.99 ppm in DMF-d_7, are absent in the 5 h spectrum (Figure 1). Furthermore, the ^{t}Bu protons are shifted upfield from 0.95 to 0.78 ppm upon formation of the putative K_3L^{tBu} species. With these results in hand, and to further avoid the presence of H_3L^{tBu} in the final reaction mixtures, isolation of K_3L^{tBu} was attempted following a procedure similar to Stavropoulos and co-workers.[35] Accordingly, addition of excess KH to a DME

DOI: 10.1021/acs.inorgchem.5b00299
Inorg. Chem. 2015, 54, 4064−4075

Scheme 1

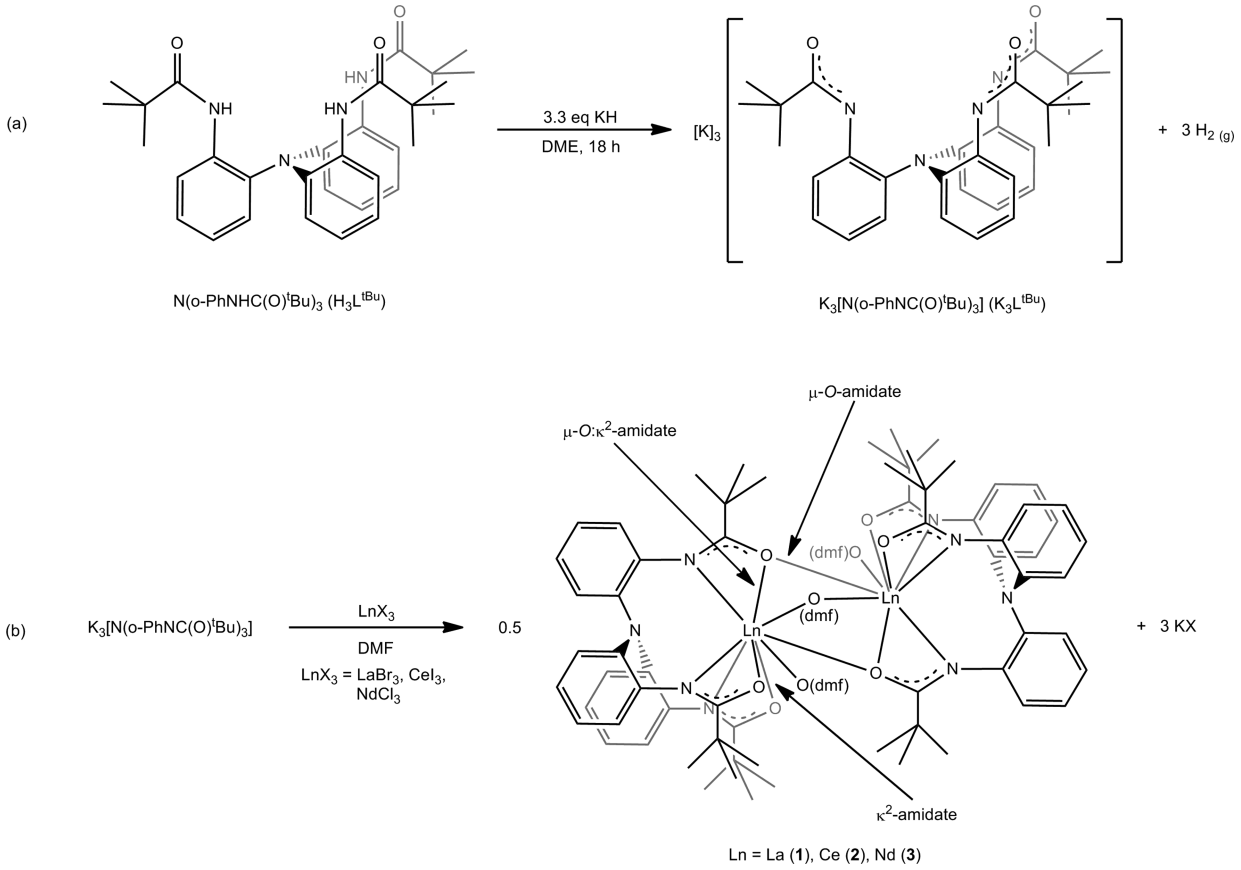

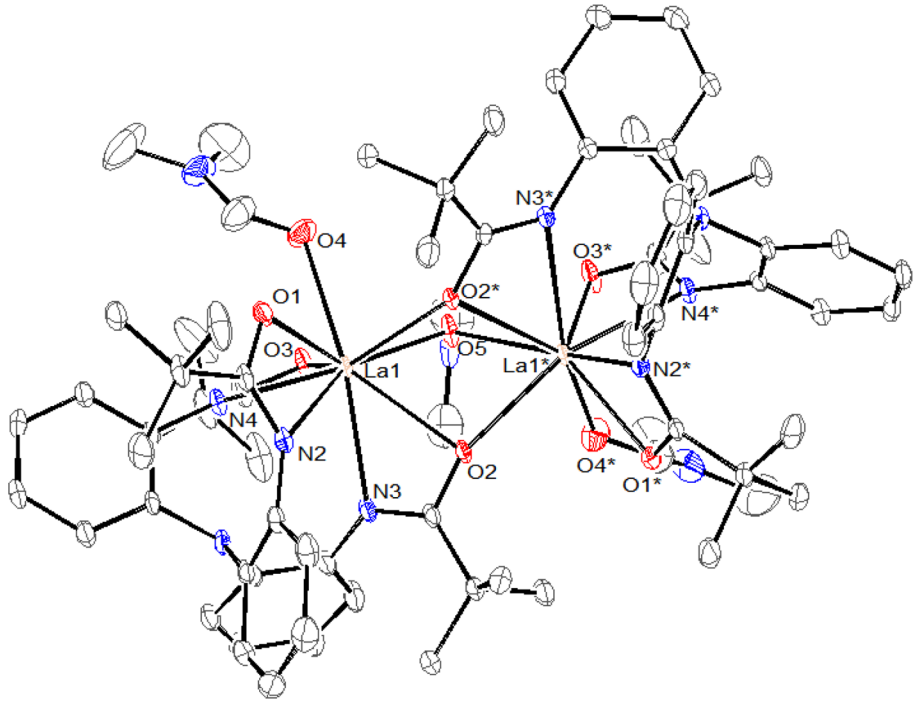

Figure 2. Solid-state molecular structure of $[La(N(o\text{-}PhNC(O)^tBu)_3)(DMF)]_2(\mu\text{-}DMF)$ (**1**) with 30% probability ellipsoids. Solvent molecules, disordered components, and hydrogen atoms omitted for clarity.

suspension of H_3L^{tBu} affords K_3L^{tBu} as a pink-peach powder in 91% yield (Scheme 1a). Like the protio derivative, this material is largely insoluble in most organic solvents but is readily solubilized by DMF. The ^1H NMR spectrum of the isolated material of K_3L^{tBu} in DMF-d_7 is spectroscopically identical to the *in situ* ^1H NMR spectrum at 5 h, exhibiting a singlet at 0.78

DOI: 10.1021/acs.inorgchem.5b00299
Inorg. Chem. 2015, 54, 4064−4075

Table 1. Selected Average Bond Distances[a] (Å) for 1·C_6H_{14}, 2·C_6H_{14}, 3·C_6H_{14}, 4·5C_6H_{14}, and 5·5C_6H_{14}

	1·C_6H_{14}	2·C_6H_{14}	3·C_6H_{14}	4·C_6H_{14}	5·C_6H_{14}
(Ln−O)κ^2-amidate	2.501(7)	2.475(8)	2.45(1)	2.41(3)[b]	2.38(2)[b]
				2.397(5)[c]	2.38(1)[c]
(Ln−O)μ-O:κ^2-amidate	2.525(2)	2.501(2)	2.53(1)	2.548(9)[b]	2.515(1)[b]
				2.610(9)[c]	2.574(8)[c]
(Ln−O)μ-O-amidate	2.610(2)	2.591(2)	2.485(6)	2.437(2)[b]	2.404(4)[b]
				2.501(6)[c]	2.475(9)[c]
(Ln−N)	2.62(2)	2.60(1)	2.56(1)	2.54(2)[b]	2.51(1)[b]
				2.57(4)[c]	2.54(4)[c]
(Ln−O)DMF/terminal	2.599(2)	2.583(2)	2.54(2)		
(Ln−O)DMF/bridging	2.608(2)	2.585(2)	2.541(1)		

[a]The error in the average bond lengths is equal to the standard deviation in the experimental values. [b]Denotes 7-coordinate metal center. [c]Denotes 8-coordinate metal center.

Table 2. X-ray Crystallographic Data for Complexes 1·C_6H_{14}, 2·C_6H_{14}, 3·C_6H_{14}, 4·5C_6H_{14}, and 5·5C_6H_{14}

	1·C_6H_{14}	2·C_6H_{14}	3·C_6H_{14}	4·5C_6H_{14}	5·5C_6H_{14}
empirical formula	$C_{81}H_{113}La_2N_{11}O_9$	$C_{81}H_{113}Ce_2N_{11}O_9$	$C_{81}H_{113}N_{11}Nd_2O_9$	$C_{162}H_{226}Ce_4N_{16}O_{12}$	$C_{162}H_{226}N_{16}Nd_4O_{12}$
crystal habit, color	block, colorless	block, pale orange	block, pale purple	block, pale orange	block, pale purple
crystal size (mm)	0.20 × 0.16 × 0.10	0.3 × 0.18 × 0.12	0.20 × 0.15 × 0.08	0.16 × 0.14 × 0.10	0.20 × 0.20 × 0.20
crystal system	monoclinic	monoclinic	triclinic	monoclinic	monoclinic
space group	$C2/c$	$C2/c$	$P\bar{1}$	$C2/c$	$C2/c$
volume (Å^3)	8156(1)	8105.6(18)	4010.6(8)	31410(10)	30895(2)
a (Å)	30.618(2)	30.497(4)	12.2127(14)	67.248(12)	67.241(3)
b (Å)	12.2582(9)	12.2527(16)	16.2838(18)	15.982(3)	15.9016(6)
c (Å)	23.3809(17)	23.360(3)	23.125(3)	30.730(6)	30.5419(16)
α (deg)	90.00	90.00	99.910(1)	90.00	90.00
β (deg)	111.653(1)	111.787(1)	103.228(1)	108.002(2)	108.905(2)
γ (deg)	99.00	90.00	111.062(1)	90.00	90.00
Z	4	4	2	8	8
formula weight (g/mol)	1662.64	1665.06	1673.30	3150.07	3166.55
density (calculated) (Mg/m^3)	1.354	1.364	1.386	1.332	1.362
absorption coefficient (mm^{-1})	1.094	1.170	1.342	1.200	1.386
F_{000}	3448	3456	1736	13104	13168
total no. reflections	45308	44668	27527	154417	241436
unique reflections	9708	9457	27527	29777	9708
R_{int}	0.0370	0.0457	0.0000 (twinned crystal)	0.0996	0.0370
final R indices [$I > 2\sigma(I)$]	R_1 = 0.0360, wR_2 = 0.0987	R_1 = 0.0370, wR_2 = 0.1018	R_1 = 0.0397, wR_2 = 0.0873	R_1 = 0.0449, wR_2 = 0.0963	R_1 = 0.0675, wR_2 = 0.1396
largest diff peak and hole (e$^-$ Å^{-3})	1.269 and −0.832	1.395 and −0.841	1.124 and −0.824	0.948 and −1.680	2.240 and −1.285
GOF	1.284	1.262	0.935	0.915	0.895

ppm, assignable to the ^{t}Bu protons (see Supporting Information, Figure S8). Lastly, as expected the amide NH stretching frequency is not observed in its solid-state IR spectrum (KBr mull) (see Supporting Information, Figure S1).[31]

With isolated K_3L^{tBu}, we attempted to synthesize the target complexes using DMF as a solvent medium in order to promote the solubility of both the ligand and the lanthanide(III) halide starting materials. The addition of 1 equiv of finely ground $LaBr_3$ to a DMF solution of K_3L^{tBu} results in formation of [La(N(*o*-PhNC(O)^{t}Bu)$_3$)(DMF)]$_2$(μ-DMF) (**1**), isolated in 64% yield as a white microcrystalline solid (Scheme 1b). Complex **1** is soluble in polar solvents such as DMF, dichloromethane, and chloroform but is only partially soluble in diethyl ether or toluene and is completely insoluble in hexanes or *n*-pentane.

The solid-state molecular structure of **1** was determined by single-crystal X-ray crystallography (Figure 2). A summary of relevant structural parameters and full crystallographic details for complex **1** can be found in Tables 1 and 2, respectively. In the solid-state, **1** crystallizes in the monoclinic centrosymmetric space group $C2/c$ as a hexane solvate. It features a dinuclear core with two 9-coordinate La(III) centers in distorted tricapped trigonal prismatic geometries. Each La center in **1**·C_6H_{14} is bound to one tris(amidate) ligand in a chelating coordination mode and one terminally bound DMF ligand coordinated through the carbonyl oxygen atom. There is also a third disordered DMF ligand which bridges both La centers through its carbonyl oxygen atom. Notably, two pendant arms of each tris(amidate) ligand bind in a κ^2-amidate fashion, while the third arm bridges the La metal centers via the oxygen atom (μ-O:κ^2-amidate and μ-O-amidate). The average O−C and N−C bond lengths, 1.29(1) Å and 1.306(6) Å, respectively, are equivalent and thus indicate significant electron delocalization through the κ^2-amidate and μ-O:κ^2-amidate backbone.[19,20] The average κ^2-amidate La−O bond distance (2.501(7) Å) appears

DOI: 10.1021/acs.inorgchem.5b00299
Inorg. Chem. 2015, 54, 4064−4075

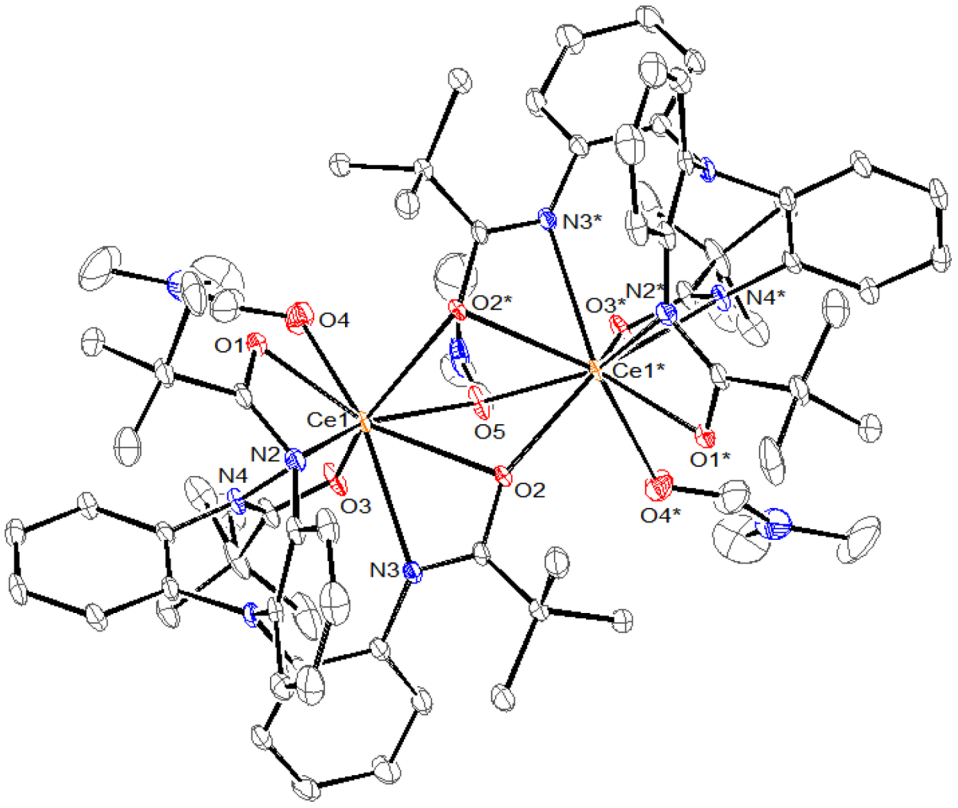

Figure 3. Solid-state molecular structure of $[Ce(N(o\text{-}PhNC(O)^tBu)_3)(DMF)]_2(\mu\text{-}DMF)]$ (**2**) with 30% probability ellipsoids. Solvent molecules, disordered components, and hydrogen atoms omitted for clarity.

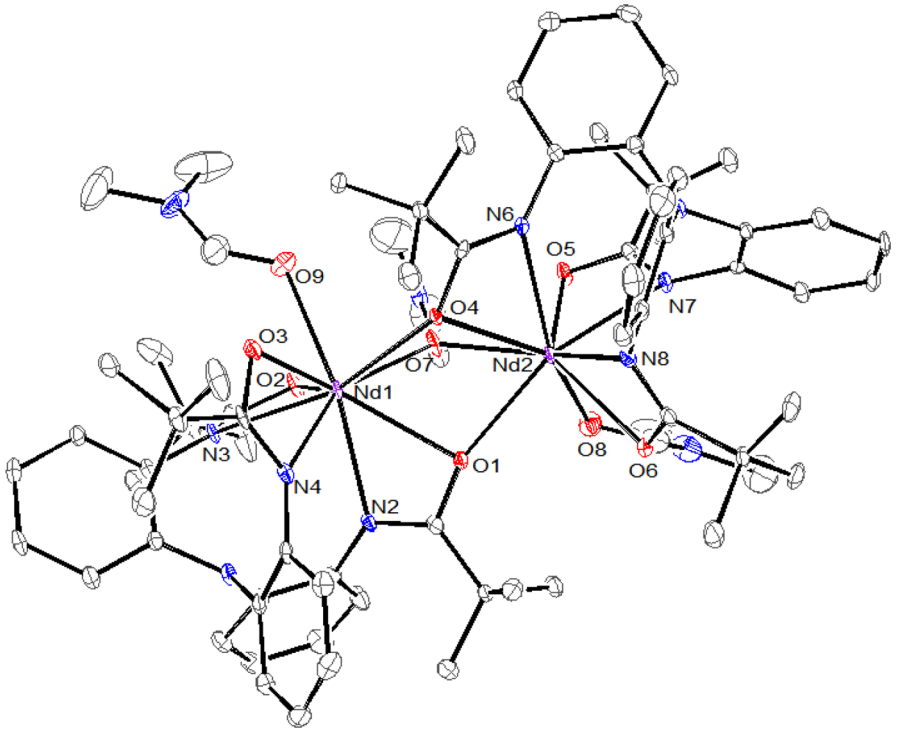

Figure 4. Solid-state molecular structure of $[Nd(N(o\text{-}PhNC(O)^tBu)_3)(DMF)]_2(\mu\text{-}DMF)$ (**3**) with 30% probability ellipsoids. Solvent molecules, disordered components, and hydrogen atoms omitted for clarity.

statistically equivalent relative to the μ-O:κ^2-amidate La−O bond distance (La1−O2 = 2.525(2) Å), and both are similar to known La−O interactions.[36−38] Not surprisingly, the μ-O-amidate interaction between O2 and the second La center (La1*−O2 = 2.610(2) Å) is longer relative to both the κ^2-amidate and μ-O:κ^2-amidate interactions. The La−O bond

DOI: 10.1021/acs.inorgchem.5b00299
Inorg. Chem. 2015, 54, 4064−4075

distance within the terminal DMF ligand (La1−O4 = 2.599(2) Å) is statistically identical to the La−O bond distance observed within the bridging DMF ligand (La1−O5 = 2.608(2) Å). Interestingly, the La−O_{DMF} bond lengths are longer relative to other La−DMF solvento complexes,[39−41] likely a function of the steric constraints imposed by the bulky tris(amidate) ligand. Lastly, as expected the average La−N bond length (2.62(2) Å) is longer relative to the κ^2-amidate and μ-O:κ^2-amidate La−O bond lengths and is typical of La−N interactions.[42−44]

Following the structural determination of **1**, we attempted to extend this chemistry to Ce and Nd with the intention of isolating a series of lanthanide tris(amidate) complexes for comparative purposes. Accordingly, addition of either CeI_3 or $NdCl_3$ to a DMF solution of K_3L^{tBu} results in formation of $[Ce(N(o\text{-}PhNC(O)^tBu)_3)(DMF)]_2(\mu\text{-}DMF)$ (**2**) or $[Nd(N(o\text{-}PhNC(O)^tBu)_3)(DMF)]_2(\mu\text{-}DMF)$ (**3**), respectively (Scheme 1b). Complex **2** can be isolated as an orange microcrystalline powder in 50% yield, while complex **3** can be isolated as a pale purple microcrystalline powder in 51% yield; both have identical solubility properties as complex **1**. Complexes **2** and **3** were structurally characterized by single-crystal X-ray crystallography, and their solid-state molecular structures can be found in Figures 3 and 4. A summary of their relevant structural parameters and full crystallographic details are tabulated in Tables 1 and 2, respectively.

In the solid-state, **2** is isostructural with **1**·C_6H_{14} crystallizing as a hexane solvate in the monoclinic centrosymmetric space group *C*2/*c*. As observed in **1**·C_6H_{14}, the average κ^2-amidate Ce−O bond distance (2.475(8) Å) in **2**·C_6H_{14} is statistically equivalent relative to the μ-O:κ^2-amidate Ce−O bond distance (Ce1−O2 = 2.501(2) Å), and both are similar to known Ce−O interactions.[45−47] Further, the μ-O-amidate interaction between O2 and the second Ce center (Ce1*−O2 = 2.591(2) Å) is significantly longer relative to both the κ^2-amidate and μ-O:κ^2-amidate interactions. Following the expected trends of the lanthanide contraction, the Ce−O bond distances are shorter relative to the La−O bond distances observed in **1**·C_6H_{14} with the exception of the κ^2-amidate bonding interactions which are statistically identical.[48] The Ce−O bond length within the terminal DMF ligand (Ce1−O4 = 2.583(2) Å) is equivalent to the Ce−O bond length observed within the bridging DMF ligand (Ce1−O4 = 2.585(2) Å) and as observed in **1**·C_6H_{14} are longer relative to other Ce−DMF solvento complexes.[49−51] Lastly, the average Ce−N bond distance (2.60(1) Å) is longer relative to both the average κ^2-amidate and μ-O:κ^2-amidate Ce−O bond distances but interestingly is equivalent to the average La−N bond distance (2.62(2) Å) observed in **1**·C_6H_{14}.

The solid-state molecular structure of complex **3** (Figure 4) exhibits identical geometry and connectivity as **1**·C_6H_{14} and **2**·C_6H_{14} but crystallizes in the triclinic centrosymmetric space group $P\bar{1}$ as a hexane solvate. In contrast to what is observed in **1**·C_6H_{14} and **2**·C_6H_{14}, the average κ^2-amidate Nd−O bond distance (2.45(1) Å) and the average μ-O-amidate Nd−O bond distance (2.485(6) Å) are equivalent and significantly shorter relative to the average μ-O:κ^2-amidate Nd−O bond distance (2.53(1) Å). The Nd−O bond distances in **3**·C_6H_{14} are comparable to other reported Nd−O bond interactions.[47,52,53] Interestingly, the average μ-O:κ^2-amidate Nd−O bond length is slightly longer than that same bond in **2**·C_6H_{14} (2.501(2) Å), and the average μ-O-amidate Nd−O bond length is much shorter than the average μ-O-amidate Ln−O bond distances in **1**·C_6H_{14} and **2**·C_6H_{14}. These bonding differences may be due to several factors including the different crystallization space group and/or the increased steric congestion about the smaller Nd(III) ion,[48] both of which may influence the crystal packing and structural metrics. However, the relatively large error values associated with **3**·C_6H_{14} may also mean that the longer average μ-O:κ^2-amidate Nd−O bond length is not particularly significant in a chemical bonding sense that requires rationalization. The average Nd−O bond distance within the terminally bound DMF ligands (2.54(2) Å) and the average Nd−O bond distance within the bridging DMF ligand (2.541(1) Å) are statistically identical and are slightly shorter relative to both **1**·C_6H_{14} and **2**·C_6H_{14}. Lastly, the average Nd−N bond length (2.56(1) Å) is equivalent to the average Ln−N bond distances observed in **1**·C_6H_{14} and **2**·C_6H_{14} and is comparable to other reported Nd−N bonding interactions.[45,52,53]

There are several lanthanide complexes containing non-multipodal amidate ligands (only one N,O group per ligand) reported in the literature, many containing ancillary cyclopentadienyl groups as supporting coligands,[21−24,26,28−30,54,55] for example, the dinuclear complex, $[Cp'_2SmOC(^nBu)NPh]_2$.[29] However, more relevant non-organolanthanide examples include the Y dinuclear tris(amidate) complex, $[Y(^tBu[O,N]\text{-}(CH_3)_2Ph)_3]_2$, reported by Schafer and co-workers.[19] Each Y center is bound to three discrete amidate ligands. Similar to **1**·C_6H_{14} - **3**·C_6H_{14}, two are in a κ^2-amidate coordination mode, and one acts as a bridging ligand to another Y atom through the amidate oxygen atom via a μ-O:κ^2-amidate interaction. Finally, Yao and co-workers recently reported the anionic, monomeric lanthanide-lithium tetra(amidate) complexes, $Li(THF)Ln\text{-}(C_6H_5C(O)NC_6H_3(^iPr)_2)_4(THF)$ (Ln = La, Nd).[20] These complexes feature four amidate ligands: one group is chelating (κ^2-amidate), two groups are chelating and bridge the metal centers (μ-O:κ^2-amidate), and another group is nonchelating but still bridges the metal centers (μ-O:μ-N-amidate). The structural determination of **1**·C_6H_{14} - **3**·C_6H_{14} reveals that dinuclear species can persist even when a bulky tripodal tris(amidate) scaffold is employed. Moreover, the isolation of **2**·C_6H_{14} is the first example of a Ce containing amidate complex; La and Nd amidates are very rare, with most amidate complexes pertaining to the middle to late 4f ions, highlighting the scarcity of coordination chemistry knowledge for early lanthanide amidate complexes.

Following structural determination, complexes **1**−**3** were characterized by ^{1}H NMR spectroscopy. The room-temperature ^{1}H NMR spectrum of **1** in C_6D_6 features two overlapping singlets at 0.99 and 1.00 ppm in a 1:2 ratio, respectively, assignable to the ^{t}Bu protons (see Supporting Information, Figure S9). On the basis of the solid-state molecular structure of **1** (*vide supra*) the observed splitting is likely a consequence of the κ^2-amidate and μ-O:κ^2-amidate interactions of the amidate pendant arms causing the ^{t}Bu protons to be in two slightly different environments. Three resonances are also observed for the DMF ligands, observed at 2.09, 2.57, and 7.93 ppm in a 3:3:1 ratio, respectively. The signals attributed to the DMF ligands differ from noncoordinated DMF in C_6D_6, thus supporting the notion that they remain coordinated to the Ln(III) centers while in solution.[56] As expected of an f^1 ion, the ^{1}H NMR spectrum of complex **2** in C_6D_6 is paramagnetically broadened and exhibits complicated splitting patterns in the range 0 to +9 ppm (see Supporting Information, Figure S11). Specifically, the ^{t}Bu protons are tentatively assignable to two broad resonances at 0.57 and 2.05 ppm in a 1:2 ratio, respectively. Furthermore, the Me protons of the DMF ligands

DOI: 10.1021/acs.inorgchem.5b00299
Inorg. Chem. 2015, 54, 4064−4075

Scheme 2

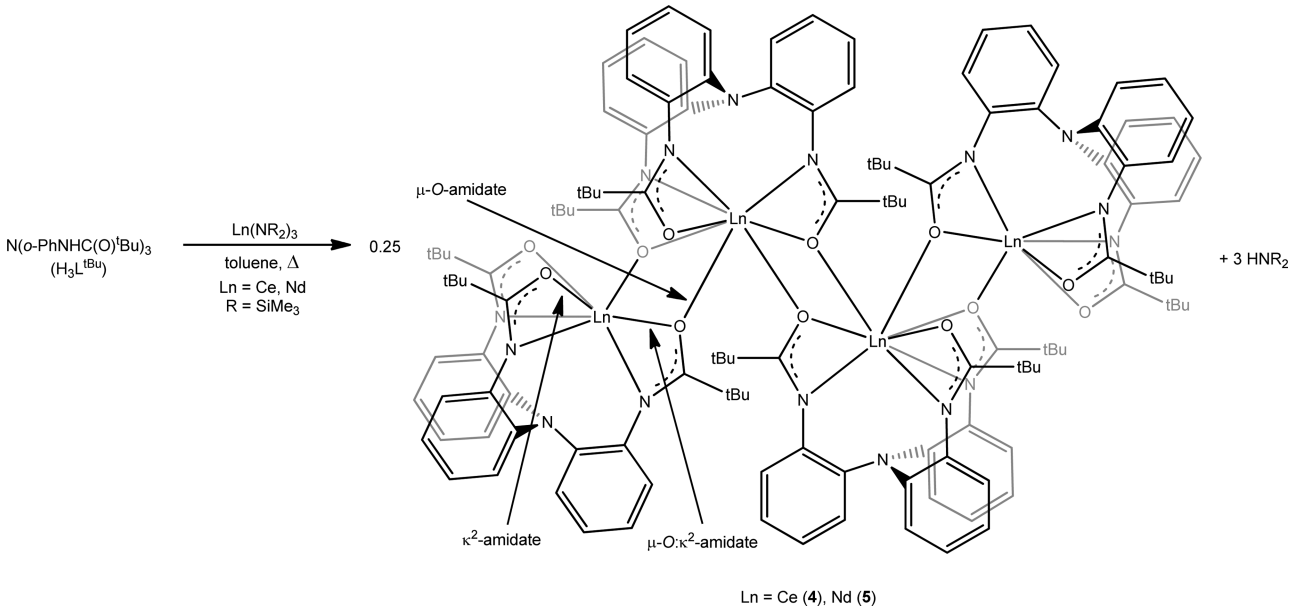

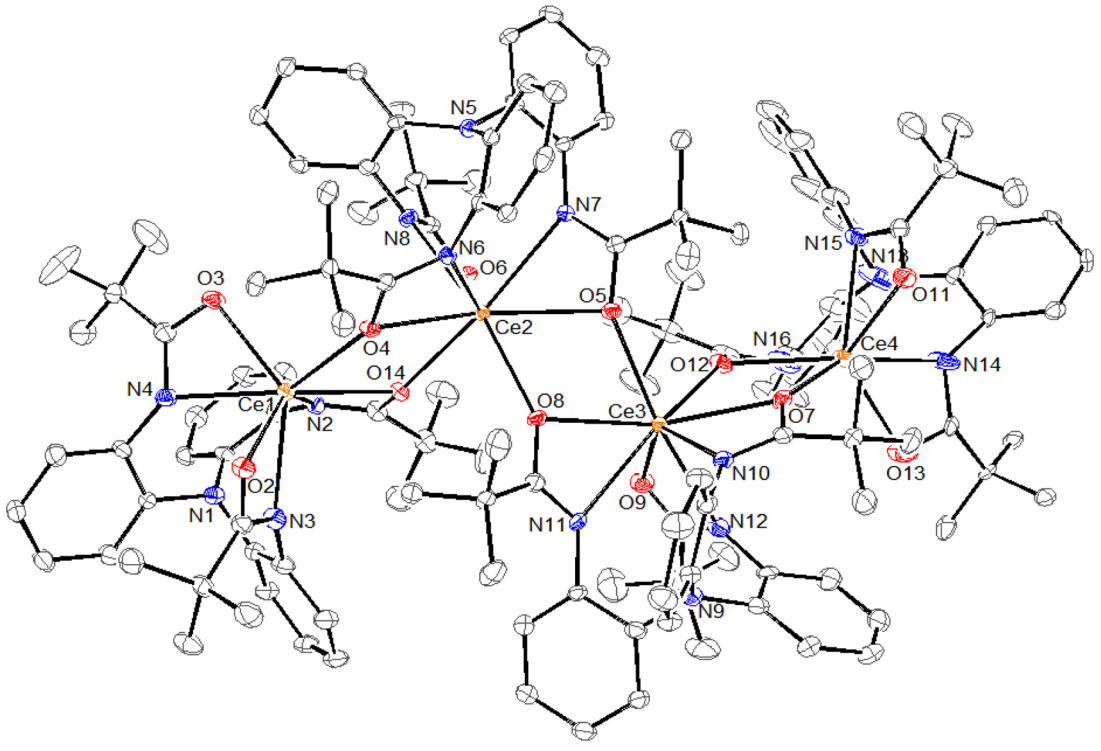

Figure 5. Solid-state molecular structure of $[Ce(N(o\text{-}PhNC(O)^tBu)_3)]_4$ (**4**) with 30% probability ellipsoids. Solvent molecules, disordered components, and hydrogen atoms omitted for clarity. Complex **5** has identical molecular connectivity (see Supporting Information, Figure S20).

are either partially overlapping with other resonances or are completely obscured. However, a well-isolated but significantly broadened resonance at 8.55 ppm is assignable to the aldehyde proton of the DMF ligands. The ^{1}H NMR spectrum of **3** is similar to **2**, featuring significant paramagnetic broadening and complicated splitting patterns in the range −1 to +11 ppm (see Supporting Information, Figure S12). Complexes **1**−**3** were further characterized by solid-state IR spectroscopy (KBr mull) which exhibit spectra similar to one another and are dominated by the stretches of the tris(amidate) ligands (see Supporting Information, Figure S2). Lastly, the UV−vis spectra of complexes **2** and **3** are typical of Ln(III) complexes, in which the electronic transitions are largely energy and line-width independent of the local ligand coordination environment about the Ln(III) center (see Supporting Information, Figures S4 and S5).[50,57−60]

The use of DMF as a reaction medium to prepare complexes **1**−**3** results in disordered solvento-bridged dinuclear complexes, thus inhibiting simple comparisons of structural metrics in pursuit of defining bonding trends across the 4f series. Therefore, we sought an alternative synthetic approach by employing a noncoordinating solvent with the goal of isolating

DOI: 10.1021/acs.inorgchem.5b00299
Inorg. Chem. 2015, 54, 4064−4075

monomeric Ln(III) tris(amidate) species via protonolysis, a method that has proven successful in similar systems.[19,20] Accordingly, addition of H_3L^{tBu} to a tol-d_8 solution of $Ce[N(SiMe_3)_2]_3$ resulted in the appearance of several new paramagnetically shifted and broadened resonances at −25.2, −13.7, 3.36, 4.93, 8.16, and 17.4 ppm over the course of several hours as observed by ^{1}H NMR spectroscopy (see Supporting Information, Figure S16). The slow reactivity is likely due to the poor solubility of H_3L^{tBu} in tol-d_8; however, upon mild heating, H_3L^{tBu} readily dissolves, and the reaction is complete within 1 h (see Supporting Information, Figure S17). With these results in hand, we sought to isolate the paramagnetic product observed in the *in situ* ^{1}H NMR spectra. Interestingly, addition of 1 equiv of H_3L^{tBu} to a toluene solution of either $Ce[N(SiMe_3)_2]_3$ or $Nd[N(SiMe_3)_2]_3$, followed by gentle heating, affords the tetranuclear complexes, $[Ln(N(o\text{-}PhNC(O)^tBu)_3)]_4$ (Ln = Ce (**4**), Nd (**5**)), respectively, rather than the anticipated monomeric product (Scheme 2).

Both complexes **4** and **5** were structurally characterized by single-crystal X-ray crystallography. The solid-state molecular structure of **4** can be found in Figure 5, while the solid-state molecular structure of **5** can be found in the Supporting Information. A summary of relevant structural parameters for complexes **4** and **5** are tabulated in Table 1, while full crystallographic details are tabulated in Table 2. Complexes **4** and **5** crystallize in the monoclinic centrosymmetric space group *C*2/*c* as hexane solvates and are isostructural. In the solid-state, **4**·$5C_6H_{14}$ and **5**·$5C_6H_{14}$ feature tetranuclear cores with two 7-coordinate Ln(III) centers in distorted trigonal prismatic geometries and two 8-coordinate Ln(III) centers in, according to Haigh's criteria, distorted dodecahedron geometries.[61] Each 7-coordinate Ln center is bound to one tripodal tris(amidate) ligand with two pendant arms in a κ^2-amidate chelating coordination mode and one arm in a μ-O:κ^2-amidate coordination mode. Each 8-coordinate Ln center is also bound to one tripodal tris(amidate) ligand but with only one pendant arm exhibiting κ^2-amidate chelation, while the other two arms are in a μ-O:κ^2-amidate coordination modes. To complete the tetranuclear structure the 7-coordinate Ln center forms an μ-O-amidate interaction with an adjacent 8-coordinate Ln ion, while each 8-coordinate Ln center has two pendant arms involved in μ-O-amidate bridging interactions: one arm forms a bridging interaction with the other 8-coordinate Ln center, and another arm forms a bridging interaction with a nearby 7-coordinate Ln center. As a consequence of this complicated multinuclear structure, some of the bond types are not equivalent between the 7- and 8-coordinate centers, and thus the Ln(III) centers will be discussed separately regarding their metrical parameters. Lastly, it should be noted, as observed in **1**·C_6H_{14}-**3**·C_6H_{14}, the average O−C and N−C bond lengths (**4**·$5C_6H_{14}$: C−O = 1.31(1) Å, C−N: 1.31(1) Å; **5**·$5C_6H_{14}$: C−O: 1.30(1) Å, C−N: 1.30(1) Å) indicate electron delocalization through the κ^2-amidate and μ-O:κ^2-amidate backbone.

In complex **4**·$5C_6H_{14}$, the 7-coordinate Ce centers exhibit an average κ^2-amidate Ce−O bond distance (2.41(3) Å) and an average μ-O-amidate Ce−O bond distance (2.437(2) Å), which are significantly shorter in comparison to the average μ-O:κ^2-amidate Ce−O bond distance (2.548(9) Å). The average Ce−N bond length (2.54(2) Å) is statistically equivalent relative to the average Ce−N bond length (2.60(1) Å) in **2**·C_6H_{14} and is comparable to previously reported Ce−N bonding interactions.[45,46,62] The 8-coordinate Ce(III) centers in **4**·$5C_6H_{14}$ exhibit similar metrical trends as the 7-coordinate Ce(III) centers. For example, both the average κ^2-amidate Ce−O bond distance (2.397(5) Å) and the average μ-O-amidate Ce−O bond distance (2.501(6) Å) are significantly shorter relative to the average μ-O:κ^2-amidate Ce−O bond distance (2.610(9) Å). The average Ce−N bond length (2.57(4) Å) of the 8-coordinate Ce centers in **4**·$5C_6H_{14}$ is equivalent to the average Ce−N bond length of the 7-coordinate Ce centers and to the Ln−N bonding interactions observed in **1**·C_6H_{14}-**3**·C_6H_{14}. Notably, both the average κ^2-amidate and μ-O-amidate Ce−O bond distances in **4**·$5C_6H_{14}$ are shorter in comparison to those same bonds in dinuclear **2**·C_6H_{14}, while the average μ-O:κ^2-amidate Ce−O bond distance in **4**·$5C_6H_{14}$ is significantly longer. These observations are likely due to the lower coordination number of the Ce(III) ions and the tetranuclear configuration of the Ce(III) nuclei in **4**·$5C_6H_{14}$, thus resulting in a less sterically congested ligand coordination environment.[8] It should also be noted that both the average μ-O:κ^2-amidate and μ-O-amidate bond distances of the 8-coordinate centers are statistically longer relative to those same bonds of the 7-coordinate centers. This may be a consequence of the larger coordination number and greater steric congestion about the 8-coordinate metal ion.

Complex **5**·$5C_6H_{14}$ exhibits similar bonding trends to the isostructural Ce tetranuclear complex. Specifically, the 7-coordinate Nd(III) centers exhibit an average κ^2-amidate Nd−O bond distance (2.38(2) Å) and an average μ-O-amidate Nd−O bond distance (2.404(4) Å) which are shorter relative to the average μ-O:κ^2-amidate Nd−O bond distance (2.515(1) Å). Furthermore, the average Nd−N bond length (2.51(1) Å) is statistically identical to the average Nd−N bond length (2.56(1) Å) in **3**·C_6H_{14}. The 8-coordinate Nd(III) centers in **5**·$5C_6H_{14}$ exhibit an average κ^2-amidate Nd−O bond distance (2.38(1) Å) and an average μ-O-amidate Nd−O bond distance (2.475(9) Å) which are also significantly shorter relative to the average μ-O:κ^2-amidate Nd−O bond distance (2.574(8) Å). As observed in **4**·$5C_6H_{14}$, both the average μ-O:κ^2-amidate and μ-O-amidate bond distances of the 8-coordinate centers are statistically longer relative to those same bonds of the 7-coordinate centers. Lastly, the average Nd−N bond length (2.54(4) Å) is statistically identical to both the average Nd−N bond length of the 7-coordinate metal centers and to **3**·C_6H_{14}.

Similar to complexes **1**−**3**, the solid-state molecular structures of **4** and **5** feature a tripodal tris(amidate) ligand with a combination of κ^2-amidate, μ-O:κ^2-amidate, and μ-O-amidate ligation modes not observed before with this particular scaffold and the transition metals. Further, the isolation and structural characterization of **4** and **5** demonstrate how a tripodal amidate ligand platform can support unprecedented tetranuclear cluster formation with the lanthanides, that are not formed with non-multipodal amidate ligands.[19−30] The absence of a coordinating solvent does not overcome the preference of large Ln(III) ions for higher coordination numbers, and it appears that despite the steric bulk of the tripodal amidate ligands mononuclear complexes are not accessible. In fact, and unpredictably, novel tetranuclear cores are formed instead in **4** and **5** containing two types of Ln(III) coordination environments with different coordination numbers (seven and eight).

Complexes **4** and **5** exhibit complicated ^{1}H NMR spectra. For example, the ^{1}H NMR spectrum of **5** in C_6D_6 features six broad and paramagnetically shifted resonances at −18.6, −11.9, 2.67, 3.77, 9.56, and 11.5 ppm in a 1:1:1:1:1:1 ratio, assignable to the ^{t}Bu protons of the amidate ligands (see Supporting Information, Figure S15). Unfortunately, the high solubility of

DOI: 10.1021/acs.inorgchem.5b00299
Inorg. Chem. 2015, 54, 4064−4075

4 in both nonpolar and ethereal solvents impedes its crystallization in meaningful yields, and beyond the isolation of a few single crystals suitable for X-ray crystallography, characterization studies of **4** were performed on the crude material. Following extraction into hexanes, the ^{1}H NMR spectrum of the crude reaction mixture containing complex **4** in C_6D_6 exhibits similar features as **5** (see Supporting Information, Figure S13). Lastly, complexes **4** and **5** were characterized by IR spectroscopy (KBr mull), featuring spectra similar to **1**−**3**, and by UV−vis spectroscopy, in which the reported spectra are typical of Ln(III) ions (see Supporting Information).[50,57−60]

Since mononuclear complexes were not formed under the reaction conditions studied, disruption of the di- and tetranuclear complexes was explored, specifically with Lewis bases, in an attempt to break up the multinuclear cores. Monitoring the addition of excess triphenylphosphine oxide (TPPO) to a DMF-d_7 solution of complex **1** by multinuclear NMR spectroscopies revealed no observable reactivity. Addition of more basic ligands such as excess acetonitrile (MeCN), pyridine or dimethylaminopyridine (DMAP) also did not reveal any observable reactivity as monitored by ^{1}H NMR spectroscopy, even over prolonged reaction times. The lack of reactivity may be a consequence of the oxophilic nature of the Ln(III) ions and/or the steric protection afforded by the bulky *tert*(butyl)-substituted amidate ligands. More likely though, especially in the case of MeCN, is the notion that certain Lewis bases weakly coordinate to the lanthanides; thus, failure to substitute the strongly coordinating DMF solvent molecules may not be unexpected.[63,64] In contrast, addition of excess DMF to a C_6D_6 solution of tetranuclear complex **5** resulted in rapid *in situ* conversion to dinuclear complex **3** as observed by ^{1}H NMR spectroscopy. Following removal of all volatiles in vacuo, the ^{1}H NMR spectrum of the crude reaction material in C_6D_6 revealed the absence of any resonances associated with complex **5** and is consistent with the formation of complex **3** (see Supporting Information, Figure S19). The observation that complex **5** is structurally disrupted by DMF but not by, if only slightly, more basic ethereal solvents (e.g., THF) is likely a consequence of DMF's high polarity and its large partial negative charge on the donating O atom, resulting in an ability to bind strongly to hard Ln(III) ions.

SUMMARY

The tripodal tris(amidate) ligand, $[N(o\text{-PhNC(O)}^t\text{Bu})_3]^{3-}$, readily coordinates to Ln(III) ions (Ln = La, Ce, Nd) with a combination of κ^2-amidate, μ-O:κ^2-amidate, and μ-O-amidate ligation modes not observed in previously reported transition metal-amidate complexes. Specifically, synthesis and isolation of the dinuclear solvento complexes, $[Ln(N(o\text{-PhNC(O)}^t\text{Bu})_3)(DMF)]_2(\mu\text{-DMF})$ (Ln = La (**1**), Ce(**2**), Nd(**3**)), were achieved in good yields by employing the lanthanide trihalide precursors in the presence of the isolated amidate salt, $K_3[N(o\text{-PhNC(O)}^t\text{Bu})_3]$, in DMF. In contrast, in noncoordinating solvents, the tetranuclear complexes, $[Ln(N(o\text{-PhNC(O)}^t\text{Bu})_3)]_4$ (Ln = Ce (**4**), Nd(**5**)), were isolated with no evidence for generation of mononuclear species under the conditions examined. The bridged multinuclear complexes synthesized, isolated and structurally characterized likely occur as a consequence of the preference of the large early Ln(III) ions to achieve higher coordination numbers compared to smaller transition metals. While the dinuclear complexes **1**−**3** highlight differences between transition metal and lanthanide amidate bonding trends with multipodal amidate scaffolds, the tetranuclear complexes **4**−**5** demonstrate how switching from simple nonpodal amidate ligands to a multipodal amidate framework provides access to novel Ln(III) amidate complexes within the 4f series. Finally, complexes **2** and **4** are the first examples of cerium coordinated to amidate ligands, helping to fill a knowledge gap regarding the coordination chemistry of the early trivalent lanthanide ions with mixed N,O donors.

EXPERIMENTAL SECTION

General. All reactions and subsequent manipulations were performed under anaerobic and anhydrous conditions either under high vacuum or in an atmosphere of high purity argon gas. Dichloromethane (DCM), diethyl ether (Et_2O), 1,2-dimethoxyethane (DME), *N*,*N*-dimethylformamide (DMF), hexanes, *n*-pentanes, tetrahydrofuran (THF), and toluene were purchased anhydrous from Sigma-Aldrich and stored over a mixture of activated 3 and 4 Å molecular sieves for at least 48−72 h before use. Benzene-d_6, *N*,*N*-dimethylformamide-d_7, and toluene-d_8 were dried over a mixture of activated 3 and 4 Å molecular sieves for at least 48 h before use. The lanthanide tris(amides), $Ln[N(SiMe_3)_2]_3$ (Ln = Ce, Nd), were prepared according to modified literature procedures (*vide infra*).[65−68] $K[N(SiMe_3)_2]$ was recrystallized from toluene before use. 2,2′,2″-tris(pivalamidotriphenyl)amine ($N(o\text{-PhNHC(O)}^t\text{Bu})_3$, H_3L^{tBu}) was prepared as previously described.[31] All other reagents were purchased from commercial suppliers and used as received.

NMR spectra were recorded on a Bruker Avance 400 MHz spectrometer. ^{1}H and ^{13}C{^{1}H} NMR spectra were referenced to external $SiMe_4$ using the residual protio solvent peaks as internal standards (^{1}H NMR experiments) or the characteristic resonances of the solvent nuclei (^{13}C NMR experiments). IR spectra were recorded on a PerkinElmer FTIR spectrometer as KBr mulls. UV−vis experiments were performed either on an Agilent 8453 UV−vis spectrometer (complexes **2** and **4**) or a Cary 5E UV−vis spectrophotometer (complexes **3** and **5**). Elemental analyses for complexes **1**−**3** were performed by the Micro-Elemental Laboratory at ALS Environmental (Columbia Analytical Services).

Synthesis of $N(o\text{-PhNKC(O)}^t\text{Bu})_3$ (K_3L^{tBu}). To a stirring suspension of $N(o\text{-PhNHC(O)}^t\text{Bu})_3$ (H_3L^{tBu}, 102 mg, 0.188 mmol) in DME (7 mL) was added excess potassium hydride (KH, 28 mg, 0.70 mmol) as an off-white/gray powder. Over the course of several hours, the solution gradually changed from a white suspension to a slightly particulated orange solution. Mild heat and vigorous bubbling was observed, presumed to be the expected hydrogen reaction byproduct. After ∼18 h, the solution turned to a heavily particulated, pink-peach solution. The pink-peach material was isolated on a medium porosity filter frit and washed with excess DME (5 mL) and DCM (6 mL) to remove unreacted H_3L^{tBu}. The material was then dried in vacuo for 2 h before use (112 mg, 91%). ^{1}H NMR (DMF-d_7, 25 °C, 400 MHz): δ 0.78 (s, 27 H, tBu), 6.26 (t, 3 H, J_{HH} = 8.0 Hz, aryl CH), 6.53 (m, 6 H, J_{HH} = 7.7 Hz, aryl CH), 7.55 (d, 3 H, J_{HH} = 7.0 Hz, aryl CH). Note: The proteo derivative of the triamidoamine ligand, $N(o\text{-PhNHC(O)}^t\text{Bu})_3$ (H_3L^{tBu}), exhibits a resonance at 8.99 ppm in its ^{1}H NMR spectrum in DMF-d_7 assignable to the NH protons. This resonance is not observed in the ^{1}H NMR spectra of the *in situ* synthesis of K_3L^{tBu} or the isolated material of K_3L^{tBu} (see the Supporting Information for corresponding spectra). IR (KBr pellet, cm^{-1}): 2967(s), 2922(2), 2867(s), 1660(w), 1650(w sh), 1589(m), 1514(s), 1443(s), 1399(s), 1360(s), 1302(sh), 1278(s), 1259(s), 1229(s), 1185(m), 1171(w), 1155(m), 1109(s), 1083(sh), 1045(m), 1025(w), 997(w), 937(s), 933(s), 904(s), 855(w sh), 844(m), 811(w), 799(w), 771(s), 752(s), 737(sh), 699(w), 678(w), 629(m), 619(sh), 553(m), 511(m), 478(w), 459(m).

Synthesis of $Ce[N(SiMe_3)_2]_3$. Finely ground $CeBr_3$ (57 mg, 0.15 mmol) was suspended in THF (1 mL) to which 2.9 equiv of $K[N(SiMe_3)_2]$ (87 mg, 0.44 mmol) was added dropwise as a THF solution (2 mL). No color change was observed with the addition. The solution was heated gently for 10 min resulting in a color change from colorless to bright yellow concomitant with the deposition of a fine white particulate. The solution was removed from heating, allowed to

DOI: 10.1021/acs.inorgchem.5b00299
Inorg. Chem. 2015, 54, 4064−4075

cool to room temperature, and filtered through a Celite column (0.5 cm × 2 cm) supported on glass wool. All volatiles were removed in vacuo, and the material was extracted into hexanes (3 mL) and filtered through a new Celite column (0.5 cm × 2 cm) supported on glass wool. All volatiles were removed in vacuo to give a bright yellow solid (75 mg, 83%). ^{1}H NMR (C_6D_6, 25 °C, 400 MHz): δ −3.46 ppm (s, 54 H, SiMe_3). By ^{1}H NMR spectroscopy, the material is spectroscopically identical to previous reports.[67,68]

Synthesis of Nd[N(SiMe$_3$)$_2$]$_3$. Finely ground $NdCl_3$ (72 mg, 0.29 mmol) was suspended in THF (2 mL) to which 2.9 equiv of K[N(SiMe_3)$_2$] (160 mg, 0.802 mmol) was added dropwise as a THF solution (2 mL). No color change was observed with the addition. The solution was heated gently for 10 min resulting in a color change from colorless to pale blue concomitant with the deposition of a fine white particulate. The solution was removed from heating, allowed to cool to room temperature, and filtered through a Celite column (0.5 cm × 2 cm) supported on glass wool. All volatiles were removed in vacuo, and the material extracted into hexanes (3 mL) and filtered through a new Celite column (0.5 cm × 2 cm) supported on glass wool. This step was repeated a second time. All volatiles were removed in vacuo to give a pale blue solid (113 mg, 68%). ^{1}H NMR (C_6D_6, 25 °C, 400 MHz): δ −6.25 ppm (s, 54 H, SiMe_3). By ^{1}H NMR spectroscopy, the material is spectroscopically identical to previous reports.[66,67]

Synthesis of [La(N(*o*-PhNC(O)^{t}Bu)$_3$)(DMF)]$_2$(μ-DMF) (1). To a pale orange solution of N(*o*-PhNKC(O)^{t}Bu)$_3$ (K_3L^{tBu}, 61 mg, 0.093 mmol) in DMF (2 mL) was added finely ground $LaBr_3$ (37 mg, 0.098 mmol) as a white crystalline powder. Upon the addition, the solution became less intense in color. Once the $LaBr_3$ was observed to be fully dissolved (∼15 min), all volatiles were removed in vacuo for ∼1.5 h until the crude material was completely dry. The material was then extracted into toluene (3 mL) and filtered through a Celite column (0.5 cm × 2 cm) supported on glass wool to give a pale yellow, almost colorless, filtrate. This filtrate was concentrated to less than 1 mL and subsequently layered with excess hexanes (∼5 mL). Storage of this solution at −35 °C for 24 h resulted in the deposition of a white microcrystalline powder (47 mg, 64%). Crystals suitable for X-ray analysis were grown from a toluene/hexanes vapor diffusion solution. Anal. Calcd for $C_{75}H_{99}La_2N_{11}O_9\cdot(C_6H_{14})$: C, 58.25; H, 6.45; N, 9.06 Found: C, 57.99; H, 6.56; N, 8.81. ^{1}H NMR (C_6D_6, 25 °C, 400 MHz): δ 0.99−1.00 (m, 54 H total, Me), 2.09 (s, 9 H, Me, DMF), 2.57 (s, 9 H, Me, DMF), 6.84 (q, 8 H, J_{HH} = 7.9 Hz, aryl CH), 6.89 (q, 10 H, J_{HH} = 7.9 Hz, aryl CH), 7.21 (t, 6 H, J_{HH} = 7.8 Hz, aryl CH), 7.93 (s, 3 H, CH, DMF). ^{13}C{^{1}H} NMR (C_6D_6, 25 °C, 100 MHz): δ 29.6 (Me), 32.3 (Me, DMF), 36.7 (Me, DMF), 41.7 (CMe), 121.8, 123.9, 125.5, 129.8, 140.6, 147.2, 165.9 (CH, DMF), 181.7 (CO). IR (KBr pellet, cm^{-1}): 1685(w), 1676(sh), 1670(sh), 1664(sh), 1655(s), 1652(sh), 1640(sh), 1634(sh), 1619(sh), 1593(m), 1578(sh), 1571(sh), 1560(s), 1543(s), 1535(s), 1511(sh), 1507(s), 1499(s), 1480(s), 1465(m), 1444(s), 1427(w), 1400(s), 1377(m), 1356(s), 1334(s), 1311(sh), 1274(m), 1218(m), 1193(m), 1190(m), 1166(sh), 1119(sh), 1101(m), 1063(sh), 1041(w), 1037(w), 944(sh), 934(m), 924(w), 908(w), 868(w), 837(w), 804(w), 753(s), 740(sh), 694(w), 669(m), 651(w), 622(m), 598(w), 585(w), 579(w), 545(w), 502(w), 481(w).

Synthesis of [Ce(N(*o*-PhNC(O)^{t}Bu)$_3$)(DMF)]$_2$(μ-DMF) (2). To a pale orange solution of N(*o*-PhNKC(O)^{t}Bu)$_3$ (K_3L^{tBu}, 57 mg, 0.088 mmol) in DMF (3 mL) was added finely ground CeI_3 (48 mg, 0.092 mmol) as a green-yellow crystalline powder. Upon the addition, the solution became less intense in color. Once the CeI_3 was observed to be fully dissolved (∼5 min), all volatiles were removed in vacuo for ∼2 h until the crude material was completely dry. The material was then extracted into toluene (4 mL) and filtered through a Celite column (0.5 cm × 2 cm) supported on glass wool to give a pale orange filtrate. All volatiles were removed in vacuo, and the material was extracted into toluene (2 mL) for a second time. The solution was filtered through a new Celite column (0.5 cm × 2 cm) supported on glass wool to give a slightly darker orange filtrate. This filtrate was concentrated to less than 1 mL and subsequently layered with excess hexanes (∼5 mL). Storage of this solution at −35 °C for 24 h resulted in the deposition of pale orange crystals (34 mg, 50%). Crystals suitable for X-ray analysis were grown from a toluene/hexanes vapor diffusion solution. Anal. Calcd for $C_{75}H_{99}Ce_2N_{11}O_9\cdot(0.5C_6H_{14})$: C, 57.76; H, 6.59; N, 9.50 Found: C, 57.95; H, 6.85; N, 8.77. ^{1}H NMR (C_6D_6, 25 °C, 400 MHz): δ 0.57 (br s, 18 H, Me), 2.05 (br s, 45 H, Me, **2** and DMF), 2.50 (br s, 9 H, Me, DMF), 5.91 (br s, 4 H, aryl CH), 6.09 (br s, 3 H, aryl CH), 6.38 (br s, 5 H, aryl CH), 7.07 (br s, 6 H, aryl CH), 7.57 (br s, 4H, aryl CH), 7.76 (br s, 2 H, aryl CH), 8.55 (br s, 3 H, CH, DMF). UV−vis (toluene, 2.6 × 10^{-5} M): λ_{max} = 295 nm. IR (KBr pellet, cm^{-1}): 1685(sh), 1678(sh), 1664(sh), 1655(s), 1651(sh), 1632(sh), 1623(w), 1594(m), 1560(m), 1542(m), 1524(s), 1494(m), 1481(s), 1460(sh), 1444(s), 1400(m), 1386(w), 1358(m), 1344(w), 1306(m), 1274(m), 1250(w), 1222(m), 1196(w), 1183(w), 1173(w), 1161(m), 1116(w), 1100(m), 1066(w), 1053(w), 1037(w), 945(w), 933(m), 910(w), 868(w), 839(w), 800(w), 768(sh), 754(s), 746(m), 693(w), 669(m), 651(w), 626(m), 598(w), 596(w), 577(w), 567(w), 545(w), 500(w), 482(w).

Synthesis of [Nd(N(*o*-PhNC(O)^{t}Bu)$_3$)(DMF)]$_2$(μ-DMF) (3). To a pale orange solution of N(*o*-PhNKC(O)^{t}Bu)$_3$ (K_3L^{tBu}, 114 mg, 0.174 mmol) in DMF (4 mL) was added finely ground $NdCl_3$ (47 mg, 0.188 mmol) as a pale purple crystalline powder. Upon the addition, the solution became less intense in color. Once the $NdCl_3$ was observed to be fully dissolved (∼10 min), all volatiles were removed in vacuo for ∼3 h until the crude material was completely dry. The material was then extracted into toluene (4 mL) and filtered through a Celite column (0.5 cm × 2 cm) supported on glass wool to give a pale purple filtrate. All volatiles were removed in vacuo, and the material was extracted into toluene (2 mL) for a second time. The solution was filtered through a new Celite column (0.5 cm × 2 cm) supported on glass wool to give a pale purple filtrate. This filtrate was concentrated to less than 1 mL and subsequently layered with excess hexanes (∼6 mL). Storage of this solution at −35 °C for 24 h resulted in the deposition of pale purple crystals (70 mg, 51%). Crystals suitable for X-ray analysis were grown from a toluene/hexanes vapor diffusion solution. Anal. Calcd for $C_{75}H_{99}N_{11}Nd_2O_9\cdot(0.5C_6H_{14})(C_7H_8)$: C, 59.27; H, 6.67; N, 8.95 Found: C, 59.22; H, 6.87; N, 8.58. ^{1}H NMR (C_6D_6, 25 °C, 400 MHz): δ 0.10 (br s, 18 H, Me), 1.57−1.74 (br m, 45 H, Me, **3** and DMF), 2.96 (s, 9 H, Me, DMF), 5.78 (br s, 4 H, aryl CH), 5.87−5.95 (br m, 6 H, aryl CH), 6.30 (br s, 3 H, aryl CH), 6.61 (br s, 4 H, aryl CH), 7.35−7.42 (br m, 7 H, aryl CH), 9.99 (br s, 3 H, CH, DMF). UV−vis (toluene, 5.1 × 10^{-3} M, nm): λ_{max} = 806, 802, 750, 744, 741, 738, 679, 598, 588, 586, 583, 578, 529, 514, 475, 462, 431. IR (KBr pellet, cm^{-1}): 1686(sh), 1659(s), 1651(sh), 1633(sh), 1622(sh), 1592(m), 1562(sh), 1549(s), 1542(s), 1496(sh), 1480(s), 1448(m), 1401(s), 1378(m), 1356(s), 1340(s), 1313(sh), 1273(m), 1219(s), 1195(s), 1191(s), 1161(sh), 1142(w), 1101(m), 1062(m), 1039(m), 946(m), 934(m), 909(m), 865(w), 836(w), 806(w), 766(sh), 753(s), 742(sh), 693(m), 669(m), 661(w), 621(m), 598(w), 585(w), 579(w), 544(w), 511(sh), 501(m), 481(w).

Synthesis of [Ce(N(*o*-PhNC(O)^{t}Bu)$_3$)]$_4$ (4). To a yellow solution of Ce(NR_2)$_3$ (R = SiMe_3, 28 mg, 0.045 mmol) in toluene (2 mL) was added N(*o*-PhNHC(O)^{t}Bu)$_3$ (H_3L^{tBu}, 27 mg, 0.050 mmol) as a white powder. No color change was observed, and H_3L^{tBu} was largely insoluble. The solution was then gently heated for ∼30 min during which H_3L^{tBu} slowly solubilized, and the solution turned to an orange color. The solution was then removed from heat, allowed to cool to room temperature, and filtered through a Celite column (0.5 cm × 2 cm) supported on glass wool to give an orange filtrate. All volatiles were removed in vacuo, and the material was extracted into hexanes (2 mL) and filtered through a new Celite column (0.5 cm × 2 cm) supported on glass wool to give a slightly darker orange filtrate. Extraction into hexanes (1 mL) was repeated for a second time. This material crystallizes poorly from hexanes, toluene, and ethereal solvents due to its extremely high solubility resulting in intractable yields. However, a small amount of pale orange crystals suitable for X-ray analysis were grown at −35 °C from a toluene/hexanes vapor diffusion solution. Except X-ray crystallography, all characterization on complex **4** was performed on the crude reaction material, isolated by removal of volatiles from the crude reaction mixture, extraction into hexanes, and filtration through a Celite column (0.5 cm × 2 cm) supported on glass wool. After exposure to reverse pressure for several

DOI: 10.1021/acs.inorgchem.5b00299
Inorg. Chem. 2015, 54, 4064−4075

hours, an orange powder was afforded (26 mg, 85% *crude*). Elemental analysis of **4** was not performed due to extremely low crystallization yields despite modifying solvent conditions, solution concentrations and temperature of crystallization. ^{1}H NMR (C_6D_6, 25 °C, 400 MHz): δ −25.56 (br s, 18 H, Me), −13.80 (br s, 18 H, Me), 3.44 (br s, 18 H, Me), 5.04 (br s, 18 H, Me), 6.62 (d, 4 H, J_{HH} = 3.0 Hz, aryl CH), 7.06 (d, 4 H, J_{HH} = 4.0 Hz, aryl CH), 7.41 (t, 4 H, J_{HH} = 7.0 Hz, aryl CH), 7.52 (t, 4 H, J_{HH} = 7.0 Hz, aryl CH), 7.62 (t, 4 H, J_{HH} = 7.0 Hz, aryl CH), 7.81 (d, 4 H, J_{HH} = 7.0 Hz, aryl CH), 8.05 (t, 4 H, J_{HH} = 6.0 Hz, aryl CH), 8.35 (br s, 18 H, Me), 8.42 (t, 4 H, J_{HH} = 7.0 Hz, aryl CH), 8.77 (d, 4 H, J_{HH} = 6.0 Hz, aryl CH), 8.92 (m, 4 H, aryl CH), 9.59 (m, 4 H, aryl CH), 10.18 (t, 4 H, J_{HH} = 6.0 Hz, aryl CH), 17.62 (br s, 18 H, Me). UV−vis (toluene, 1.2 × 10^{-5} M): λ_{max} = 298 nm. IR (KBr pellet, cm^{-1}): 1686(sh), 1655(m), 1660(sh), 1645(sh), 1634(w), 1594(m), 1560(sh), 1542(sh), 1555(s), 1498(w), 1481(s), 1445(s), 1400(s), 1376(w), 1355(m), 1334(sh), 1318(m), 1274(m), 1247(sh), 1218(m), 1195(sh), 1184(m), 1158(sh), 1118(sh), 1101(w), 1040(w), 1032(w), 934(s), 913(m), 840(m), 803(w), 766(sh), 755(s), 742(sh), 699(w), 669(w), 656(w), 623(w), 587(w), 544(w), 505(w), 493(w).

Synthesis of [Nd(N(*o*-PhNC(O)^{t}Bu)$_3$)]$_4$ (5). A toluene suspension of N(*o*-PhNHC(O)^{t}Bu)$_3$ (H_3L^{tBu}, 28.2 mg, 0.052 mmol) (2 mL) was heated until it formed a colorless solution (∼45 min). Upon cooling to room temperature, 0.9 equiv of Nd(NR$_2$)$_3$ (R = SiMe$_3$, 28.6 mg, 0.046 mmol) was added as a pale blue powder. A slight color change to pale purple was observed after an additional 30 min of stirring at room temperature. The solution was then filtered through a Celite column (0.5 cm × 2 cm) supported on glass wool to give a pale purple filtrate. All volatiles were removed in vacuo, and the material was extracted into hexanes (4 mL) and filtered over a new Celite column (0.5 cm × 2 cm) supported on glass wool. All volatiles were removed in vacuo, and the material was extracted into Et_2O (1 mL) and filtered a third time. The filtrate was concentrated to less than 1 mL and set up as a reverse vapor diffusion with hexanes (∼2 mL). Storage of this solution at −35 °C for 24 h resulted in the deposition of pale purple crystals suitable for X-ray analysis (20 mg, 64%). Even with multiple crystallizations, a persistent impurity of unknown formulation was observed at ∼0.3 ppm in the ^{1}H NMR spectra of the crystals inhibiting characterization by elemental analysis. ^{1}H NMR (C_6D_6, 25 °C, 400 MHz): δ −18.61 (br s, 18 H, Me), −11.94 (br s, 18 H, Me), 2.67 (br s, 18 H, Me), 3.77 (br s, 18 H, Me), 4.76 (m, 4 H, aryl CH), 5.15 (s, 2 H, aryl CH), 5.55 (s, 2 H, aryl CH), 6.14−6.37 (m, 12 H, aryl CH), 6.88 (m, 4 H, aryl CH), 7.04 (t, 2 H, J_{HH} = 6.0 Hz, aryl CH), 7.51−7.60 (m, 16 H, aryl), 8.58 (s, 2 H, aryl CH), 8.77 (s, 2 H, aryl CH), 8.84 (s, 2 H, aryl CH), 9.56 (br s, 18 H, Me), 11.48 (br s, 18 H, Me). UV−vis (toluene, 2.5 × 10^{-3} M, nm): λ_{max} = 808, 804, 752, 747, 742, 738, 682, 601, 590, 588, 582, 580, 529, 516, 478, 465, 434. IR (KBr pellet, cm^{-1}): 1687(sh), 1655(w), 1642(w), 1589(sh), 1544(s), 1494(sh), 1480(s), 1447(s), 1400(s), 1378(m), 1356(s), 1334(sh), 1320(s), 1272(s), 1218(s), 1193(sh), 1183(s), 1155(sh), 1120(sh), 1101(m), 1040(m), 1033(sh), 945(sh), 933(s), 908(s), 860(w), 835(w), 799(w), 767(sh), 753(s), 738(sh), 693(m), 669(w), 647(w), 621(m), 597(w), 584(m), 541(w), 500(m), 479(w).

X-ray Crystallography. Data for **1**·C_6H_{14}, **2**·C_6H_{14}, **3**·C_6H_{14}, **4**·5C_6H_{14}, and **5**·5C_6H_{14} were collected on a Bruker AXS SMART APEX II charge coupled-device (CCD) diffractometer, equipped with graphite monochromatized MoKα X-ray source (α = 0.7107 Å). Crystals of **1**·C_6H_{14}, **2**·C_6H_{14}, **3**·C_6H_{14}, and **4**·5C_6H_{14} were mounted in a nylon cryoloop using Paratone-N oil under argon gas, and all data were collected at a temperature of 120(1) K with a Cryo Industries of America Cryocool G2 cooling device. A crystal of **5**·5C_6H_{14} was mounted onto a plastic loop from a pool of Fluorolube and immediately placed in a cold N_2 vapor stream. A hemisphere of data was collected using ω scans with 0.3° frame widths and 10 s frame exposures for **1**·C_6H_{14}, **2**·C_6H_{14}, **3**·C_6H_{14}, **4**·5C_6H_{14}, and **5**·5C_6H_{14}. Data collection and cell parameter determination were conducted using APEX II software.[69] Integration of data frames, including Lorentz-polarization corrections, and final cell parameter refinement were performed using SAINT$^+$ software.[70] The data were corrected for absorption using the SADABS program.[71] Decay of reflection intensity was monitored via analysis of redundant frames. The structure was solved using direct methods and difference Fourier techniques. All hydrogen atom positions were idealized and rode on the atom they were attached to. Structure solution, refinement, graphics, and creation of publication materials were performed using SHELXTL.[72] The program PLATON-SQUEEZE was used to remove disordered solvent molecules from the unit cell where appropriate, and details are in the crystallographic files.[73] A summary of relevant crystallographic data for **1**·C_6H_{14}, **2**·C_6H_{14}, **3**·C_6H_{14}, **4**·5C_6H_{14}, and **5**·5C_6H_{14} is presented in Table 2.

■ ASSOCIATED CONTENT

Supporting Information

Crystallographic details (as CIF files) for **1**·C_6H_{14}, **2**·C_6H_{14}, **3**·C_6H_{14}, **4**·5C_6H_{14}, and **5**·5C_6H_{14} and spectral data for **1**−**5**. This material is available free of charge via the Internet at http://pubs.acs.org.

■ AUTHOR INFORMATION

Corresponding Authors

*E-mail: gaunt@lanl.gov.

*E-mail: cora.macbeth@emory.edu.

Notes

The authors declare no competing financial interest.

■ ACKNOWLEDGMENTS

Lanthanide chemistry and characterization was performed under a U.S. Department of Energy, Office of Science, Basic Energy Sciences, Early Career Program award (contract DE-AC52-06NA25396). J.L.B. thanks the G. T. Seaborg Institute at Los Alamos National Laboratory for a Postdoctoral Fellowship. We also thank Timothy J. Boyle from Sandia National Laboratories for obtaining the crystallographic data for complex **5**·5C_6H_{14} and the grateful use of the Bruker X-ray diffractometer via the National Science Foundation CRIF:MU award to Prof. Kemp of the University of New Mexico (CHE04-43580).

■ REFERENCES

(1) Gong, Y.; Tian, G.; Rao, L.; Gibson, J. K. *Inorg. Chem.* **2014**, *53*, 12135.

(2) Ingram, K. I. M.; Kaltsoyannis, N.; Gaunt, A. J.; Neu, M. P. *J. Alloys Compd.* **2007**, *444*−*445*, 369.

(3) Madic, C.; Lecomte, M.; Baron, P.; Boullis, B. *C. R. Phys.* **2002**, *3*, 797.

(4) Mehdoui, T.; Berthet, J.-C.; Thuery, P.; Ephritikhine, M. *Chem. Commun.* **2005**, 2860.

(5) Lee, H. B.; Bogart, J. A.; Carroll, P. J.; Schelter, E. J. *Chem. Commun.* **2014**, *50*, 5361.

(6) Jordens, A.; Cheng, Y.-P.; Waters, K. E. *Miner. Eng.* **2013**, *41*, 97.

(7) Rapko, B. M.; McNamara, B. K.; Rogers, R. D.; Broker, G. A.; Lumetta, G. J.; Hay, B. P. *Inorg. Chem.* **2000**, *39*, 4858.

(8) Gaunt, A. J.; Reilly, S. D.; Enriquez, A. E.; Scott, B. L.; Ibers, J. A.; Sekar, P.; Ingram, K. I. M.; Kaltsoyannis, N.; Neu, M. P. *Inorg. Chem.* **2008**, *47*, 29.

(9) Edelmann, F. T. *Coord. Chem. Rev.* **2015**, *284*, 124.

(10) Bunzli, J.-C. G. *J. Coord. Chem.* **2014**, *67*, 3706.

(11) Wilson, J. J.; Birnbaum, E. R.; Batista, E. R.; Martin, R. L.; John, K. D. *Inorg. Chem.* **2015**, *54*, 97.

(12) Negri, R.; Baranyai, Z.; Tei, L.; Giovenzana, G. B.; Platas-Iglesias, C.; Benyei, A. C.; Bodnar, J.; Vagner, A.; Botta, M. *Inorg. Chem.* **2014**, *53*, 12499.

(13) Yakovenko, M. V.; Cherkasov, A. V.; Fukin, G. K.; Cui, D.; Trifonov, A. A. *Eur. J. Inorg. Chem.* **2010**, 3290.

(14) Schnaars, D. D.; Batista, E. R.; Gaunt, A. J.; Hayton, T. W.; May, I.; Reilly, S. D.; Scott, B. L.; Wu, G. *Chem. Commun.* **2011**, *47*, 7647.

DOI: 10.1021/acs.inorgchem.5b00299
Inorg. Chem. 2015, 54, 4064−4075

(15) Schnaars, D. D.; Gaunt, A. J.; Hayton, T. W.; Jones, M. B.; Kirker, I.; Kaltsoyannis, N.; May, I.; Reilly, S. D.; Scott, B. L.; Wu, G. *Inorg. Chem.* **2012**, *51*, 8557.
(16) Xiao, C.-L.; Wang, C.-Z.; Yuan, L.-Y.; Li, B.; He, H.; Wang, S.; Zhao, Y.-L.; Chai, Z.-F.; Shi, W.-Q. *Inorg. Chem.* **2014**, *53*, 1712.
(17) Marie, C.; Miguirditchian, M.; Guillaumont, D.; Tosseng, A.; Berthon, C.; Guilbaud, P.; Duvail, M.; Bisson, J.; Guillaneux, D.; Pipelier, M.; Dubreuil, D. *Inorg. Chem.* **2011**, *50*, 6557.
(18) Marie, C.; Miguirditchian, M.; Guillaneux, D.; Bisson, J.; Pipelier, M.; Dubreuil, D. *Solvent Extr. Ion. Exch.* **2011**, *29*, 292.
(19) Stanlake, L. J. E.; Beard, J. D.; Schafer, L. L. *Inorg. Chem.* **2008**, *47*, 8062.
(20) Hu, X.; Lu, C.; Wu, B.; Ding, H.; Zhao, B.; Yao, Y.; Shen, Q. *J. Organomet. Chem.* **2013**, *732*, 92.
(21) Zheng, P. Z.; Hong, J. Q.; Liu, R. T.; Zhang, Z. X.; Pang, Z.; Weng, L. H.; Zhou, X. G. *Organometallics* **2010**, *29*, 1284.
(22) Zhang, J.; Zhou, X. G.; Cai, R. F.; Weng, L. H. *Inorg. Chem.* **2005**, *44*, 716.
(23) Thomson, J. A.; Schafer, L. L. *Dalton Trans.* **2012**, *41*, 7897.
(24) Zhang, F.; Zhang, J.; Song, H.; Zi, G. *Inorg. Chem. Commun.* **2011**, *14*, 72.
(25) Wang, Q. W.; Zhang, F. R.; Song, H. B.; Zi, G. F. *J. Organomet. Chem.* **2011**, *696*, 2186.
(26) Evans, W. J.; Fujimoto, C. H.; Ziller, J. W. *Organometallics* **2001**, *20*, 4529.
(27) Wang, Y. R.; Shen, Q.; Wu, L. P.; Zhang, Y.; Sun, J. *J. Organomet. Chem.* **2001**, *626*, 176.
(28) Stanlake, L. J. E.; Schafer, L. L. *Organometallics* **2009**, *28*, 3990.
(29) Zhou, X. G.; Zhang, L. B.; Zhu, M.; Cai, R. F.; Weng, L. H. *Organometallics* **2001**, *20*, 5700.
(30) Zhang, C.; Lin, Y.; Chen, Z.; Zhou, X. *J. Rare Earth* **2006**, *24*, 9.
(31) Jones, M. B.; Hardcastle, K. I.; MacBeth, C. E. *Polyhedron* **2010**, *29*, 116.
(32) Jones, M. B.; Newell, B. S.; Hoffert, W. A.; Hardcastle, K. I.; Shores, M. P.; MacBeth, C. E. *Dalton Trans.* **2010**, *39*, 401.
(33) Jones, M. B.; Hardcastle, K. I.; Hagen, K. S.; MacBeth, C. E. *Inorg. Chem.* **2011**, *50*, 6402.
(34) Jones, M. B.; MacBeth, C. E. *Inorg. Chem.* **2007**, *46*, 8117.
(35) Celenligil-Cetin, R.; Paraskevopoulou, P.; Dinda, R.; Staples, R. J.; Sinn, E.; Rath, N. P.; Stavropoulos, P. *Inorg. Chem.* **2008**, *47*, 1165.
(36) Fuller, C. C.; Molzahn, D. K.; Jacobson, R. A. *Inorg. Chem.* **1978**, *17*, 2138.
(37) Brayshaw, P. A.; Hall, A. K.; Harrison, W. T. A.; Harrowfield, J. M.; Pearce, D.; Shand, T. M.; Skelton, B. W.; Whitaker, C. R.; White, A. H. *Eur. J. Inorg. Chem.* **2005**, 1127.
(38) Li, J.-R.; Bu, X.-H.; Zhang, R.-H. *Eur. J. Inorg. Chem.* **2004**, 1701.
(39) Berthet, J.-C.; Thuéry, P.; Ephritikhine, M. *Polyhedron* **2006**, *25*, 1700.
(40) Wang, Y.-L.; Jiang, Y.-L.; Liu, Q.-Y.; Tan, Y.-X.; Wei, J.-J.; Zhang, J. *CrystEngComm* **2011**, *13*, 4981.
(41) Stojanovic, M.; Robinson, N. J.; Chen, X.; Sykora, R. E. *Inorg. Chim. Acta* **2011**, *370*, 513.
(42) Mazzanti, M.; Wietzke, R.; Pécaut, J.; Latour, J.-M.; Maldivi, P.; Remy, M. *Inorg. Chem.* **2002**, *41*, 2389.
(43) Wietzke, R.; Mazzanti, M.; Latour, J.-M.; Pecaut, J. *J. Chem. Soc., Dalton Trans.* **1998**, 4087.
(44) Frechette, M.; Bensimon, C. *Inorg. Chem.* **1995**, *34*, 3520.
(45) Campello, M. P. C.; Lacerda, S.; Santos, I. C.; Pereira, G. A.; Geraldes, C. F. G. C.; Kotek, J.; Hermann, P.; Vaněk, J.; Lubal, P.; Kubíček, V.; Tóth, É.; Santos, I. *Chem. – Eur. J.* **2010**, *16*, 8446.
(46) Hubert-Pfalzgraf, L. G.; El Khokh, N.; Daran, J.-C. *Polyhedron* **1992**, *11*, 59.
(47) Li, Z.-Y.; Zhang, Z.-M.; Dai, J.-W.; Huang, H.-Z.; Li, X.-X.; Yue, S.-T.; Liu, Y.-L. *J. Mol. Struct.* **2010**, *963*, 50.
(48) Shannon, R. *Acta Crystallogr. A* **1976**, *32*, 751.
(49) Kozieł, M.; Pełka, R.; Rams, M.; Nitek, W.; Sieklucka, B. *Inorg. Chem.* **2010**, *49*, 4268.
(50) Seidel, C.; Lorbeer, C.; Cybińska, J.; Mudring, A.-V.; Ruschewitz, U. *Inorg. Chem.* **2012**, *51*, 4679.
(51) Mishra, S.; Jeanneau, E.; Bulin, A.-L.; Ledoux, G.; Jouguet, B.; Amans, D.; Belsky, A.; Daniele, S.; Dujardin, C. *Dalton Trans.* **2013**, *42*, 12633.
(52) Deacon, G. B.; Feng, T.; C. R. Hockless, D.; C. Junk, P.; W. Skelton, B.; H. White, A. *Chem. Commun.* **1997**, 341.
(53) Miyashita, Y.; Sanada, M.; Islam, M. M.; Amir, N.; Koyano, T.; Ikeda, H.; Fujisawa, K.; Okamoto, K. *Inorg. Chem. Commun.* **2005**, *8*, 785.
(54) Wang, Q.; Zhang, F.; Song, H.; Zi, G. *J. Organomet. Chem.* **2011**, *696*, 2186.
(55) Wang, Y.; Shen, Q.; Wu, L.; Zhang, Y.; Sun, J. *J. Organomet. Chem.* **2001**, *626*, 176.
(56) Fulmer, G. R.; Miller, A. J. M.; Sherden, N. H.; Gottlieb, H. E.; Nudelman, A.; Stoltz, B. M.; Bercaw, J. E.; Goldberg, K. I. *Organometallics* **2010**, *29*, 2176.
(57) Darroudi, M.; Hakimi, M.; Sarani, M.; Kazemi Oskuee, R.; Khorsand Zak, A.; Gholami, L. *Ceram. Int.* **2013**, *39*, 6917.
(58) Forcha, D.; Brown, K. J.; Assefa, Z. *Spectrochim. Acta, Part A* **2013**, *103*, 90.
(59) Wang, J.; Tanner, P. A. *J. Lumin.* **2008**, *128*, 1846.
(60) Duvail, M.; Ruas, A.; Venault, L.; Moisy, P.; Guilbaud, P. *Inorg. Chem.* **2010**, *49*, 519.
(61) Haigh, C. W. *Polyhedron* **1995**, *14*, 2871.
(62) Dröse, P.; Hrib, C. G.; Edelmann, F. T. *Acta Crystallogr. E* **2010**, *66*, m1386.
(63) Bodizs, G.; Helm, L. *Inorg. Chem.* **2015**, *54*, 1974.
(64) Kimura, T.; Nagaishi, R.; Kato, Y.; Yoshida, Z. *J. Alloys Compd.* **2001**, *323*−*324*, 164.
(65) Bradley, D. C.; Ghotra, J. S.; Hart, F. A. *J. Chem. Soc., Dalton Trans.* **1973**, 1021.
(66) Dash, A. K.; Razavi, A.; Mortreux, A.; Lehmann, C. W.; Carpentier, J.-F. *Organometallics* **2002**, *21*, 3238.
(67) Edleman, N. L.; Wang, A.; Belot, J. A.; Metz, A. W.; Babcock, J. R.; Kawaoka, A. M.; Ni, J.; Metz, M. V.; Flaschenriem, C. J.; Stern, C. L.; Liable-Sands, L. M.; Rheingold, A. L.; Markworth, P. R.; Chang, R. P. H.; Chudzik, M. P.; Kannewurf, C. R.; Marks, T. J. *Inorg. Chem.* **2002**, *41*, 5005.
(68) Hitchcock, P. B.; Hulkes, A. G.; Lappert, M. F.; Li, Z. *Dalton Trans.* **2004**, 129.
(69) *SMART Apex II*, 1.08 ed.; Bruker AXS, Inc.: Madison, WI, 2003.
(70) *SAINT*, 7.06 ed.; Bruker AXS, Inc.: Madison, WI, 2003.
(71) Sheldrick, G. M.; *SADABS*; 2.03 ed.; University of Gottingen, Germany, 2001.
(72) *SHELXTL PC*, 5.10 ed.; Bruker AXS, Inc.: Madison, WI, 1997.
(73) Spek, A. L. *J. Appl. Crystallogr.* **2003**, *36*, 7.

DOI: 10.1021/acs.inorgchem.5b00299
Inorg. Chem. 2015, 54, 4064−4075